Lattice dynamics of commensurate and incommensurate K_2SeO_4

J. D. Axe, M. Iizumi,* and G. Shirane
Brookhaven National Laboratory, Upton, New York 11973
(Received 27 February 1980)

K_2SeO_4 undergoes an incommensurate structural transformation at $T_0 = 128$ K followed by a commensurate "lock-in" transformation at $T_c = 93$ K. Below T_0, the soft-phonon mode associated with the transformation is "split" into modes representing fluctuations in amplitude and phase of the complex order parameter. We have studied the dispersion and temperature dependence of these modes at $T \leq 118$ K. We have also seen intensity anomalies which can be explained by interactions between a transverse-acoustic-phonon branch and the low-lying "phason" branch.

I. INTRODUCTION

The past few years have witnessed a growing interest in materials in which the crystalline translational symmetry is destroyed by small distortions of the lattice with a period incommensurate with that of the underlying lattice structure. In certain quasi-one-dimensional metals[1] such as Pt-complex salts or salts of conjugated organic ions, and in the layered d^1-metal dichalcogenides,[2] the distortions result from a Fermi-surface instability leading to an electronic charge-density wave (CDW) to which the lattice is coupled. The specification of the distortion requires a complex order parameter, $\eta_0 e^{i\phi_0}$, describing its amplitude, η_0, and phase, ϕ_0. One of the consequences of the incommensurability of a plane-wave distortion with the lattice is that no choice of ϕ_0 is energetically favored over another, and this leads naturally to the concept of phase fluctuations as elementary excitations of the distorted phase with frequencies which go to zero in the long-wavelength limit and an acousticlike dispersion relation. These phase fluctuations (or "phasons"[3] or "Fröhlich modes"[4]) should possess several novel features, but there is at present little direct evidence for their existence. Structure present in the low-temperature phonon spectra of $K_2Pt(CN)_4Br_{0.3}{\cdot}xH_2O$(KCP) seen in infrared,[5] and neutron scattering[6,7] experiments have been attributed to CDW phase fluctuations. But the situation is complicated by impurity-pinning effects and the lack of true long-range order and there seem to be unresolved difficulties[6] in this interpretation.

We have recently performed a neutron scattering study of an incommensurate lattice instability in K_2SeO_4.[8] There are two successive transformations. The first, at $T_0 = 128$ K is a second-order transformation from a high-temperature orthorhombic Pnam structure to a sinusoidally modulated one with wave vector $\vec{q}_0 \approx 0.3/\vec{a}^*$. At $T_c = 93$ K, the modulation wave vector changes discontinuously to $\vec{q}_c = \frac{1}{3}\vec{a}^*$, and the structure remains commensurate at lower temperatures. Figure 1 shows the phonon dispersion for the lowest-lying transverse modes propagating in the [100] direction at several temperatures above T_0. [The Σ_2 and Σ_3 modes are continuous at the zone boundary and it is therefore convenient to use an extended (doubled) Brillouin zone, in which the soft-mode instability now appears in the vicinity of $q = \frac{2}{3} q_{max}$.] In contrast to the CDW metals studied thus far by inelastic neutron scattering,[6-8] K_2SeO_4 shows essentially complete phonon softening, $\omega_q \to 0$ as $T \to T_0$, with relatively small damping, and consequently is a good candidate for study of the excitations below T_0. The results of such experiments are the subject of this paper. This study complements the light scattering studies which have been recently reported by Wada *et al.*,[9] Caville *et al.*,[10] and Fleury, Chiang, and Lyons.[11]

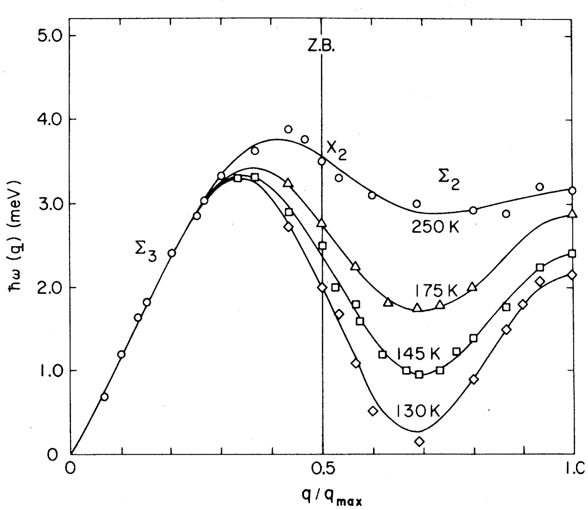

FIG. 1. Dispersion of the soft-phonon branch of K_2SeO_4 above $T_0 = 128$ K in an extended-zone scheme, from Ref. 8 (note the symmetry designation changes from Σ_3 to Σ_2 at the zone boundary) ($\vec{q}$ measured in units of a^*).

II. PHASE- AND AMPLITUDE-FLUCTUATION MODES

The low-temperature data were obtained by conventional triple-axis spectroscopy at the Brookhaven High Flux Beam Reactor using pyrolytic graphite filters with either the initial or scattered neutron energy held fixed at 14 meV. The resolution was varied through the use of appropriate combinations of 10–40 min horizontal collimators. Although many of the data were taken below T_c, where a reciprocal-lattice vector $\vec{a}_L^* = \frac{1}{3}\vec{a}^*$ could be used, we prefer to retain the high-temperature basis vectors throughout. The sample was oriented in the $(h0l)$ scattering plane and the majority of the measurements were performed along the line $(\xi, 0, 4)$ with $|\xi| \le 1.5$. The line contains a strong normal-phase reflection (0,0,4) as well as strong primary satellite reflections at or near $(\pm\frac{4}{3}, 0, 4)$. At room temperature $a^* = 0.828$ Å^{-1}.

A result of neutron scattering measurements is shown in Fig. 2 in which the excitation of phase- and amplitude-fluctuation modes gives rise to scattering peaks. As $\xi = h \pm \frac{1}{3}$ corresponds to the new zone center in the commensurate phase, each peak position of Fig. 2 gives the frequency of phase and amplitude modes at $q = 0$, which we will call ω_ϕ and ω_η, respectively. The temperature dependence of the frequencies below T_0 was measured and the results are given in Fig. 3, where they are compared with the Raman-scattering results of Wada *et al.*[9] Agreement between neutron and all the Raman results[9–11] is excellent over the temperature range for which the neutron data exist. Near T_0 $(15\ \mathrm{K} \ge T_0 - T \ge 0\ \mathrm{K})$ Fleury *et al.* report some deviations from the smooth extrapolation of the data of Wada *et al.* shown in Fig 3. The frequencies of the soft Σ_2 phonon above T_0 at $\vec{q}_0 = 0.31a^*$ are also shown in the same figure.

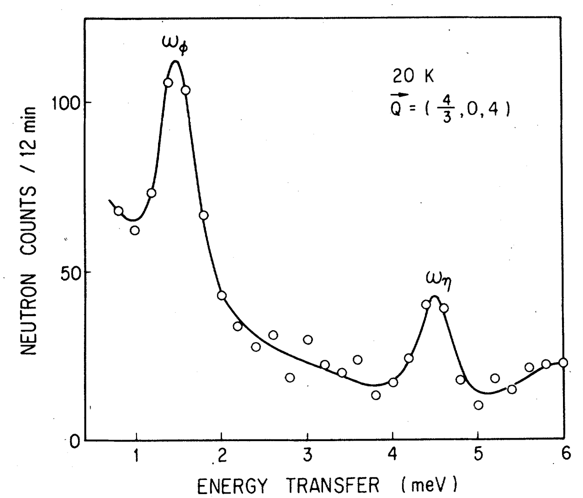

FIG. 2. Neutron scattering spectrum at $\vec{Q} = (\frac{4}{3}, 0, 4)$ at 20 K. The two peaks represent $\vec{q} = 0$ phase and amplitude-fluctuation modes.

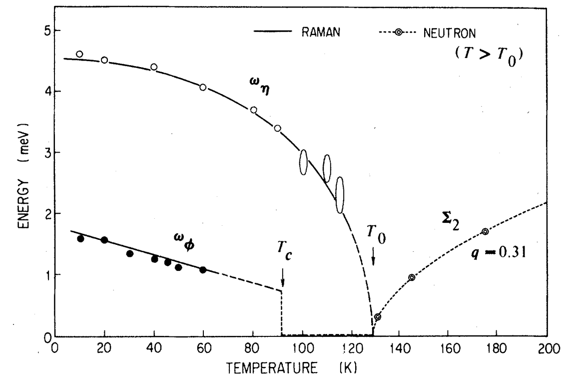

FIG. 3. Temperature dependence of $\vec{q} = 0$ phase and amplitude mode frequencies. Solid lines indicate Raman-scattering results (Ref. 9), data points are neutron results. Neutron scattering data above T_0 (Ref. 8) are also shown. The dashed portions of the ω_ϕ curve is entirely schematic, serving to indicate that ω_ϕ is expected to vanish at T_c.

The q dependence of the modes was measured at the temperature 40 K, which is in the commensurate phase, and is shown in Fig.4. The dispersion relations are shown in the completely extended zone scheme in (a) and doubly extended zone scheme in (b). The point $\frac{1}{3}h$ (h an integer) is zone center and $(\frac{1}{3}h + \frac{1}{6})$ is zone boundary. Figure 4 (a) is convenient to use to compare the results with the dispersion curve in the high-temperature phase shown in Fig. 1. The single continuous dispersion curve above T_0 splits into a number of disconnected branches. This is because the dispersion relations are shown in

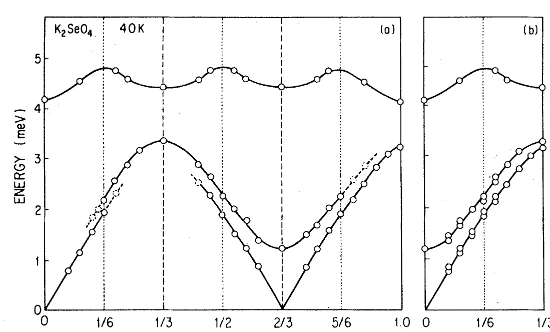

FIG. 4. Dispersion of (in order of increasing energy) transverse-acoustic, phase, and amplitude-fluctuation branches at 40 K. (a) The fully extended zone (comparable to Fig. 1). (b) The zone folded back into an irreducible doubly extended zone of the low-temperature structure.

the figure as they were actually observed in the extended zone. Some parts of branches are not observable because of the structure factor in the scattering cross section and the intensity of the scattering is transferred from one mode to another.

Trisection of the zone below T_c means that from the point of view of phonon frequencies, Fig. 4(a) can be folded back on itself along the lines $\vec{q}=\frac{1}{3}\vec{a}^*$ and $\vec{q}=\frac{2}{3}\vec{a}^*$. Figure 4(b) shows this result. Triple splitting of the single branch on one hand and the trisection of the zone on the other hand conserve the number of independent phonon modes in the crystal. The splitting of the dispersion relations below T_0 is of course a consequence of the interaction between the modes with the different q in the high-temperature zone but the same q in the low-temperature zone. This is illustrated schematically in Fig. 5. The dispersion curve of the high-temperature phase shown in (a) is repeated in (b) by taking $-\frac{2}{3}$, $\frac{2}{3}$, and $\frac{4}{3}$ as origins. Then the lattice modulation generated below T_0 causes the interaction between the branches at their crossing points. Therefore, we obtain a schematical result shown in (c) which is comparable to the observed result given in Fig. 4.

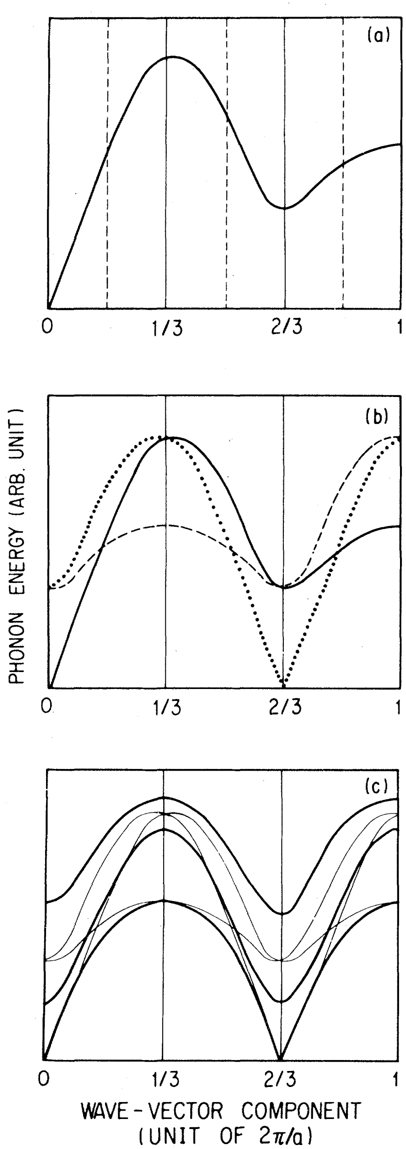

FIG. 5. (a)–(c) Schematic illustration showing how the interactions due to the static modulations cause the splitting of the single branch above T_0.

As the temperature is raised from 40 K toward $T_c=93$ K, ω_ϕ decreases and the acoustic and phason branches [the lowest two branches of Fig. 4(b)] nearly superimpose. As a result of this accidental near-degeneracy, we have been unable to unambiguously measure the behavior of the phason branch as $T\rightarrow T_c$ from below or in the incommensurate phase. Fleury *et al.*[11] report that the phason mode becomes overdamped in the region $3\geq(T_c-T)\geq 0$ K, and fail to detect a gapless phason mode in the incommensurate phase. They conclude that, at small q, the phason branch has either much-reduced Raman-scattering strength or a considerable width in the incommensurate phase. Thus the behavior of the phason branch in the incommensurate phase seems beyond the present reach of either neutron or Raman scattering in this system. Note that we take the word "phason" to be synonymous with "phase-fluctuation mode" and therefore continue to use this term to describe excitations of the commensurate phase. It is, of course, only in the incommensurate phase that the $\vec{q}=0$ phason has the added significance of being the gapless Goldstone mode.

III. ACOUSTIC-PHONON–PHASON INTERACTION

Figure 6 shows the low-energy portion of three phonon scans, taken in the low-temperature commensurate phase at $T=40$ K, near the strong superlattice reflection at $\vec{Q}=(\pm\frac{4}{3},0,4)$. In terms of the extended Brillouin zone shown in Fig. 1, Fig 6(b) represents $\xi=(q/q_{\max})=\xi_c=\frac{2}{3}$, whereas in Figs. 6(a) and 6(c) $\xi=\pm\xi_c+0.1$, respectively. The wave vectors at which the data were taken were (nearly) symmetrically disposed about the $\vec{a}^*$ axis to minimize differences in spectrometer focusing. Moreover, the crystal symmetry imposes on the scattering law the condition $\mathcal{S}(H,K,L)=\mathcal{S}(-H,K,L)$, so that the data of Figs. 6(a) and 6(c) are equivalent to data taken at $\vec{Q}=(\xi_c\pm 0.1,0,4)$, but under identical focusing conditions. The data clearly demonstrate a reversal of intensity between the lower and upper branch, the former ("acoustic") branch being the more intense for $\xi=\xi_c+0.1$, and less intense for $\xi=\xi_c-0.1$.

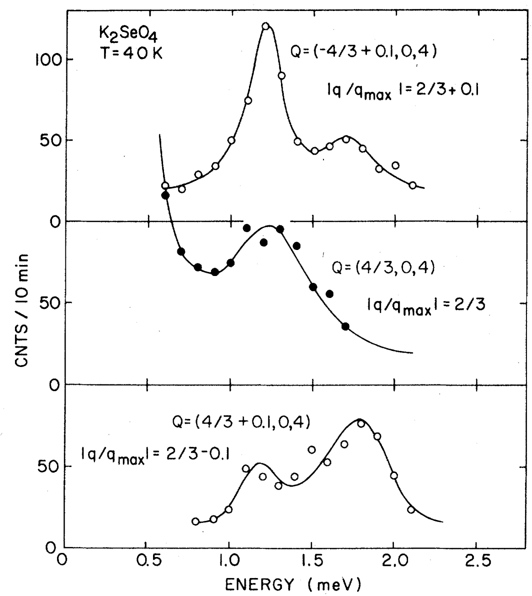

FIG. 6. The relative intensity of the Σ_3 (*xy* shear) mode and Σ_2 (phason) mode reverse for small displacements in $\vec{q}$ away from $\vec{q}=0$ (center figure).

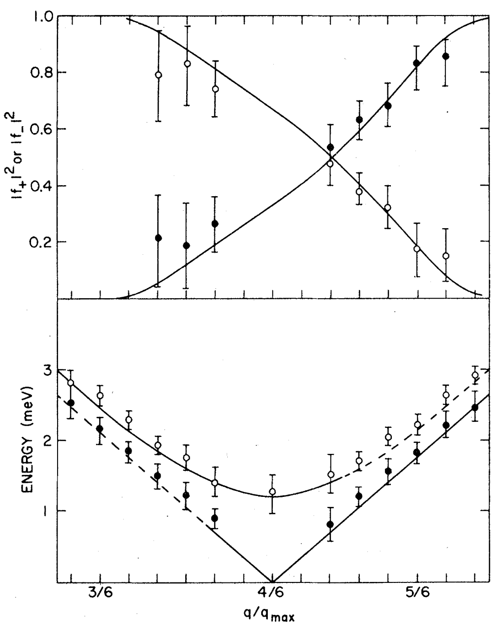

FIG. 7. Summary of interaction between Σ_2 and Σ_3 branches at $T=40$ K. (a) mode frequencies. (b) normalized-mode intensities.

Figure 7(a) summarizes the frequency dispersion of the two lowest branches near ξ_c. Note that both branches are, within experimental error, symmetric about ξ_c, whereas above T_0 the dispersion is noticeably asymmetric (see Fig. 1). The scattering *cross section,* however, is asymmetric about ξ_c as shown in Fig. 7(b), where trivial thermal occupation effects have been removed and a convenient normalization introduced by defining reduced inelastic structure factors, $f_\pm(q)$,

$$I_\pm(\vec{Q}) = [1+n(\omega_\pm)]\mathfrak{N}|f_\pm(\vec{q})|^2 \ . \qquad (1)$$

Here $I_\pm$ and $\omega_\pm$ are the integrated intensities of the scattering and frequency of the upper and lower branches, respectively, and $\mathfrak{N}$ is chosen so that $|f_+(\vec{q})|^2+|f_-(\vec{q})|^2=1$.

This sort of intensity reversal is the signature of phonon eigenvector changes that result from phonon-phonon interactions which are antisymmetric in $\vec{q}$. They have been studied most intensively in connection with piezoelectric ferroelectrics.[12] Bruce and Cowley[13] have recently discussed phason—acoustic-phonon interraction, a complication which is ignored in most treatments of phason dynamics. Since we believe that Fig. 7 represents the first observations of these effects, we have made a semiquantitative analysis of these data in order to further judge the credibility of this interpretation and to estimate the size of the interaction in K_2SeO_4.

The most important interaction responsible for renormalizing the soft excitations with $\vec{q}\approx\vec{q}_0$ below T_0 is a scattering involving the *square* of the static displacements which thus mixes plane-wave modes with wave vectors differing by $2\vec{q}_0$. Representing the normal coordinates of these normal-state phonon modes by Q_{q_0+q} and Q_{-q_0+q}, respectively, the new modes below T_0 in the vicinity of q_0 are described by[13,14]

$$Q_\eta(q) = (1/\sqrt{2})(Q_{q_0+q}+Q_{-q_0+q}) \ , \qquad (2a)$$

$$Q_\phi(q) = (1/\sqrt{2})(Q_{q_0+q}-Q_{-q_0+q}) \ . \qquad (2b)$$

These new modes represent fluctuations in amplitude and phase, respectively, of the mean sinusoidal modulation.

Iizumi *et al.*[8] have considered the role of strain as a secondary order parameter in K_2SeO_4-type systems. By a slight extension of their arguments, it is easy to show that in the commensurate phase, symmetry allows interactions between Q_{q_0+q} and Q_q, where Q_q is the normal coordinate of a low-lying transverse-acoustic mode on the soft "branch" shown in Fig. 1. (Note that for small q, Q_q transforms like Σ_3, whereas $Q_{\pm q_0+q}$ transforms like Σ_2.) This interaction is also proportional to the square of static displacements but is linear in q and is thus capable of producing the antisymmetric effects discussed above.[14] Considering only the limited manifold of three low-lying modes discussed above the quasiharmonic equations of motion become

$$\omega_q^2 \vec{U}_q = \underline{M}(q)\vec{U}_q, \quad \vec{U}_q = \begin{pmatrix} Q_{q_0+q} \\ Q_{-q_0+q} \\ Q_q \end{pmatrix} \tag{3}$$

and the dynamical matrix $\underline{M}$ has the form

$$\underline{M}(q) = \begin{pmatrix} \alpha & \beta & \gamma \\ \beta & \alpha & -\gamma \\ \gamma & -\gamma & \epsilon \end{pmatrix} , \tag{4}$$

where

$$\alpha = \tfrac{1}{2}\left(\omega_\eta^2 + \omega_\phi^2\right) + \lambda^2 q^2 , \tag{5a}$$

$$\beta = \tfrac{1}{2}\left(\omega_\eta^2 - \omega_\phi^2\right) , \tag{5b}$$

$$\gamma = Dq ; \quad \epsilon = v^2 q^2 . \tag{5c}$$

Here ω_η and ω_ϕ are the $q=0$ frequencies of the amplitude- and phase-fluctuation modes, which are known by direct experiment. λ is a constant characterizing the dispersion of the soft Σ_2 branch near $\vec{q}_0$ whose approximate value can be obtained from Fig. 1.[15] v is the velocity of the acoustic phonons above T_0, also obtained from the $\vec{q} \approx 0$ behavior of Fig. 1. In the notation of Ref. 8, D, which parametrizes the Σ_2-Σ_3 mode interaction, equals $-B_s\eta_0^2$.

Using the transformation of Eq. (2) to transform $\underline{M}(q)$ to a new basis, we find that the amplitude mode decouples, and we are left with an elementary 2×2 matrix coupling the phason and acoustic phonon

$$\underline{M}'(q) = \begin{pmatrix} \omega_\phi^2 + \lambda^2 q^2 & \sqrt{2}Dq \\ \sqrt{2}Dq & v^2 q^2 \end{pmatrix} . \tag{6}$$

Equation (6) provides a relation for fitting the dispersion of the two low-lying branches shown in Fig. 7(a) with a single disposable parameter D. Such a fit is shown by the lines in this figure, where $(\sqrt{2}D/\omega_\phi v) = 0.25$ (the value $\lambda = 0.77v$ was deduced from Fig. 1). The fit is quite satisfactory. In order to progress to a calculation of the intensity anomaly one must first discuss the one-phonon structure factors $F_{\phi,a}(\vec{Q})$ for the bare phason and acoustic modes. Fortunately, both are very simply related to F_0, the structure factor of the soft Σ_2 mode above T_0

$$F_0(\vec{Q}) = \sum_k (\vec{Q}\cdot\vec{\xi}_k) b_k e^{i\vec{Q}\cdot\vec{R}_k} ,$$

where $\vec{\xi}_k$, b_k, and $\vec{R}_k$ specify the mode eigenvector, scattering length and position within the unit cell of the k th atom. The transformation of Eq. (2) shows immediately that $F_\phi(\vec{Q}) = (2)^{-1/2}F_0(\vec{Q})$. On the other hand, the bare acoustic-mode structure factor is proportional to the elastic structure factor of the nearby Bragg peak from which it arises. For first-order satellites, the elastic structure factor is itself proportional to $F_0(\vec{Q})$. Specifically $F_a(\vec{Q}) = (2)^{-1/2}\eta_0(\vec{Q}\cdot\vec{\xi}_a)F_0(\vec{Q})$, where $\vec{\xi}_a$ is a unit polarization vector for the acoustic mode under consideration (along $\vec{c}^{\,*}$ in the present case). This proportionality is extremely useful for it means that the (unknown) complex structure factor $F_0(\vec{Q})$ can be scaled out of the expressions for the reduced structure factors $f_\pm(\vec{q})$ defined in Eq. (1). Introducing the quantities

$$\underline{f}(\vec{q}) = \begin{pmatrix} f_+ \\ f_- \end{pmatrix} \text{ and } \underline{f}^0 = (1+\Delta^2)^{-1/2}\begin{pmatrix} 1 \\ \Delta \end{pmatrix} ,$$

where $\Delta = \eta_0(\vec{Q}\cdot\vec{\xi}_a)$, the desired relation is simply

$$\underline{f}(\vec{q}) = \underline{S}(\vec{q})\cdot\underline{f}^0 ,$$

where $\underline{S}(\vec{q})$ is the eigenvector matrix which diagonalizes $\underline{M}(\vec{q})$.

The lines drawn through the data points in Fig. 7(b) represent a calculation with $\Delta \equiv [F_a(\vec{Q})/F_\phi(\vec{Q})]$ set equal to $1/\sqrt{2}$ which provides a reasonably good fit. η_0 and thus Δ could in principle be derived from precise low-temperature crystallographic data. Unfortunately, such data do not exist. However, the amplitudes of the atomic displacements implied by this value of Δ are $\lesssim 0.2$ Å, which seems quite reasonable, particularly when compared with low-temperature displacement amplitudes ~ 0.3 Å reported in Rb_2ZnBr_4, which is, in essential respects, closely similar to K_2SeO_4.

Thus we believe we have a plausible internally consistent explanation of these anomalous intensity effects which suggests that there are rather large phason–xz-shear-phonon interactions in K_2SeO_4. {We find, for example, that the limiting xz-shear sound velocity at 40 K is reduced by the factor $[1-(2D^2/\omega_\phi^2 v^2)]^{1/2} = 0.87$ from its value, v, above T_0.} It would appear to be very interesting to take advantage of this interaction in order to study indirectly the behavior of the phason mode in the incommensurate phase by ultrasonic studies.

ACKNOWLEDGMENTS

We wish to thank Y. Ishibashi and Y. Takagi for useful discussions and exchange of information. Research at Brookhaven was supported by the Division of Basic Energy Sciences, Department of Energy, under Contract No. DE-AC02-76CH00016.

*Present address: Japan Atomic Energy Research Institute, Tokai, Japan.

[1]See, for example, *Highly Conducting One-Dimensional Solids*, edited by J. Devreese (Plenum, New York, 1979).
[2]See, for example, J. A. Wilson, F. J. Di Salvo, and S. Mahajan, Adv. Phys. 24, 117 (1975).
[3]A. W. Overhauser, Phys. Rev. B 3, 3173 (1971).
[4]H. Fröhlich, Proc. R. Soc. London Ser. A 223, 296 (1954).
[5]P. Brüesch, S. Strassler, and R. Zeller, Phys. Rev. B 12, 219 (1975).
[6]R. Comès, B. Renker, L. Pintschovius, R. Currat, W. Gläser, and G. Schreiber, Phys. Status Solidi B 71, 171 (1975).
[7]K. Carneiro, G. Shirane, S. A. Werner, and S. Kaiser, Phys. Rev. B 13, 4258 (1976).
[8]M. Iizumi, J. D. Axe, G. Shirane, and K. Shimaoka, Phys. Rev. B 15, 4392 (1977).
[9]M. Wada, A. Sawada, Y. Ishibashi, and Y. Takagi, J. Phys. Soc. Jpn. 42, 1229 (1977); M. Wada, H. Uwe, A. Sawada, Y. Ishibashi, Y. Takagi, and T. Sakudo, *ibid.* 43, 544 (1977).
[10]C. Caville, V. Fawcett, and D. A. Long, in *Proceedings of the Fifth International Conference on Raman Spectroscopy, Freiburg* (Flammarion, Paris, 1976), p. 626.
[11]P. A. Fleury, S. Chiang, and K. B. Lyons, Solid State Commun. 31, 279 (1979).
[12]R. A. Cowley, Phys. Rev. Lett. 36, 744 (1976).
[13]A. D. Bruce and R. A. Cowley, J. Phys. C 11, 3609 (1978).
[14]J. D. Axe, *Proceedings of Gatlinburg Neutron Scattering Conference*, CONF-760601-P1 (U.S. Dept. of Commerce, 1976), p. 353. Bruce and Cowley (Ref. 12) discuss a different coupling which is *linear* in the static displacements and which is in general allowed by translational symmetry. One can show by point-symmetry arguments that such terms vanish for phason modes with $\vec{q} \parallel \vec{a}^*$ in K_2SeO_4 although they do produce a coupling between the amplitude fluctuations and *longitudinal*-acoustic phonons.
[15]We have simplified the description of the soft-mode dispersion and, in particular, neglect its anisotropy around $\vec{q}_0$, so that λ refers to an average value. This can be justified because the amplitude gap $\omega_+(0) >>$ (anisotropy in dispersion)q.